

MOLECULAR DYNAMICS SIMULATION OF PRIMARY IRRADIATION DEFECT FORMATION IN FE-CR ALLOYS—J.-H. Shim, H.-J. Lee, and B. D. Wirth (University of California, Berkeley)

OBJECTIVE

The objective of this work was to determine the effect of Cr on primary defect production in high-energy displacement cascades in Fe-10%Cr alloys, using two different parameterizations for the Fe-Cr interatomic potential that effectively treated the Cr atom as an oversized and undersized substitutional solute atom, respectively.

SUMMARY

Molecular dynamics simulations of displacement cascades up to 20 keV have been performed in Fe and Fe-10%Cr using two different parameterizations of Finnis-Sinclair type interatomic potentials. The two different potentials describe the extremes of positive (attractive) and negative (repulsive) binding between substitutional Cr atoms and Fe self-interstitial atoms. The effect of Cr, regardless of potential, has a minimal effect on the collisional stage of cascade and on the distribution and number of vacancy and self-interstitial atom clusters. The quantity of mixed Fe-Cr dumbbells is sensitive to the choice of potential, however.

PROGRESS AND STATUS

Introduction

9–12% Cr ferritic/martensitic steels are strong candidates for first-wall and breeding-blanket structural materials in future fusion reactor systems. Therefore, fundamental understanding of microstructural evolution under conditions of fusion neutron irradiation is important, since microstructural changes control mechanical behavior and performance. The modeling of primary defect formation by displacement cascades is a natural starting point in predicting neutron irradiation damage. Molecular dynamics (MD) simulations based on reliable semi-empirical many-body interatomic potentials have long been recognized as the most appropriate tool for the study of displacement cascades. To date many investigations have performed MD cascade simulations in pure Fe using a variety of interatomic potentials [1–4]. Cascade simulations in Fe alloys have seldom been studied, because reliable interatomic potentials for Fe alloys are limited.

Specifically considering the Fe-Cr system, there are a couple of displacement cascade simulation studies that have been recently performed [5,6]. Malerba et al. [5] performed MD cascade simulations of pure Fe and Fe-10%Cr with kinetic energies of primary knock-on atom (PKA) E_p of up to 15 keV. They employed embedded atom method (EAM) potentials to simulate the cascades. While they took the Cr potential from the work of Farkas et al. [8], they fit new Fe and Fe-Cr cross potentials to available physical properties. Their results show that Cr atoms do not have a significant influence on the collision stage of cascades and the number of surviving defects. But on the other hand, they observed mixed Fe-Cr dumbbells form preferentially in Fe-10%Cr alloys. However, the Fe potential used in that work makes the $\langle 111 \rangle$ dumbbell more stable than $\langle 110 \rangle$ dumbbell [9], opposite to experimental observations [10], recent ab-initio [11,12] and most semi-empirical potential calculations [13–15]. Meanwhile, Wallenius et al. [6] recently fit Fe-Cr EAM potentials to various physical properties of pure Fe, pure Cr and Fe-Cr alloys and simulated displacement cascades of pure Fe, Fe-5%Cr and Fe-20%Cr with E_p of up to 20 keV. Though the potentials of Wallenius et al. [6] are evidently improved by correctly predicting the stability of the dumbbells, the calculated formation energy of the Fe $\langle 110 \rangle$ and $\langle 111 \rangle$ dumbbells is more than two times larger than the recent ab-initio calculations [11,12] and the experimental data [16].

The purpose of this study is to construct two different Fe-Cr potentials, with a systematic variation in Cr behavior, and to perform MD simulations to elucidate the effect of Cr atoms in Fe on primary irradiation defect formation in displacement cascades.

Interatomic Potentials and Simulation Methods

The Finnis-Sinclair (F-S) potential [17], which provides a similar framework to the EAM potential [7], was chosen to construct the Fe-Cr potentials. In the framework of the Finnis-Sinclair formalism, the total energy of the system of the n atom system is given by:

$$E_{tot} = \frac{1}{2} \sum_{i \neq j}^n V_{ij}(R_{ij}) - \sum_i^n \left\{ \sum_j^n \phi_{ij}(R_{ij}) \right\}^{1/2} \quad (1)$$

where V_{ij} and f_{ij} are the pairwise repulsive and the many-body cohesive interactions, respectively, between atoms i and j separated by a distance R_{ij} .

The potentials for the pure elements were taken from the literature [14,17]. For Fe and Cr, the potentials of Ackland et al. [14] and Finnis and Sinclair [17], respectively, were employed. For radiation damage studies, it is important to validate a potential at very short atomic separations as well as at equilibrium separation, because atoms tend to become very close in high-energy cascades. For instance, it is known that the Fe potential developed by Finnis and Sinclair [17] is too 'soft' at short atomic separations for high-energy cascades. Calder and Bacon [1], therefore, modified this potential to make it 'stiffer' in their cascade simulations. Fortunately, the F-S Fe potential proposed later by Ackland et al. [14] was already proven to be in good agreement with the universal equation of state [18] at short atomic separations. It also turned out that the potential of Ackland et al. [14] correctly predict the stability and defect formation energy of Fe dumbbells. The volume-energy curve of the Cr potential by Finnis and Sinclair [17] is plotted in order to decide whether or not this Cr potential is relevant for high-energy cascades (Fig. 1). The agreement with the universal equation of state is quite good. Therefore, there is no need to modify the Cr potential at short atomic distances. It is also beneficial that the F-S Cr potential shows a smaller positive Cauchy pressure compared to the previous EAM Cr potentials, since it is experimentally known that Cr has a negative Cauchy pressure [6].

To construct the Fe-Cr cross potential, the two terms V_{FeCr} and f_{FeCr} must be determined. The scheme proposed by Konishi et al. [19] was adopted from the various cross potential schemes. According to this approach, the two terms are given by:

$$\phi_{FeCr} = \alpha \sqrt{\phi_{FeFe} \phi_{CrCr}} \quad (2)$$

$$V_{FeCr} = \frac{\beta}{2} \left(\frac{\phi_{FeCr}}{\phi_{FeFe}} V_{FeFe} + \frac{\phi_{FeCr}}{\phi_{CrCr}} V_{CrCr} \right) \quad (3)$$

where α and β are adjustable parameters.

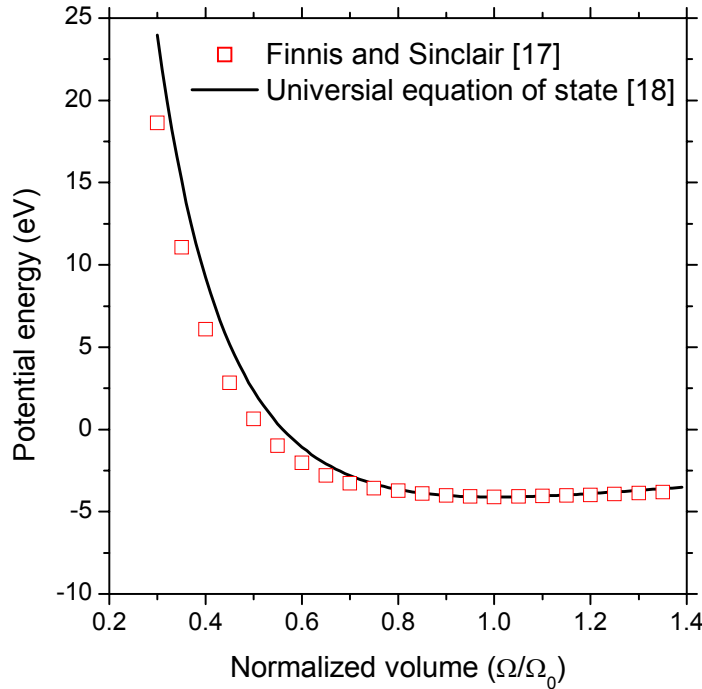


Fig. 1. Calculated potential energy versus normalized volume for Cr by the F-S potential in comparison with the universal equation of state.

Table 1. Parameters for the Fe-Cr potential fitted in this study

	α	β
FeCr I	1.00	1.25
FeCr II	0.94	0.90

In this study, α and β were fit to experimental data, including the enthalpy of mixing and lattice constants in Fe-Cr alloys. The fit parameters are provided in Table 1. The first cross-potential involved only a fit of β with α fixed equal to 1, because it is more similar to the original F-S alloy scheme proposed by Ackland and Vitek [20]. This potential was named FeCr I. FeCr I shows very good agreement with the CALPHAD calculation for the enthalpy of mixing [21], which is derived from experimental data [22], as shown in Fig. 2. Concerning the lattice constants of Fe-Cr alloys, the FeCr I potential is in agreement with experimental measurements [23–25], as shown in Fig. 3. The binding energies of various point defects are presented in Table 2. The binding energies of Fe-Cr $\langle 110 \rangle$ and $\langle 111 \rangle$ mixed dumbbells, with respect to an isolated Fe dumbbell and a well-separated Cr atom, are negative, which means that these dumbbells are not energetically stable compared to the Fe-Fe dumbbells. However, this is opposite to the recent ab-initio calculation predicting zero and positive binding energies for the $\langle 110 \rangle$ and $\langle 111 \rangle$ mixed dumbbells, respectively [26]. The Fe-Cr potential of Wallenius et al. [6] predicts a relatively large positive binding energy of 0.27 eV for the $\langle 110 \rangle$ mixed dumbbell. Further, Maury and co-workers have suggested a small (≈ 0.15 eV) positive binding energy for mixed Fe-Cr dumbbells in Fe-Cr alloys, based on experimentally

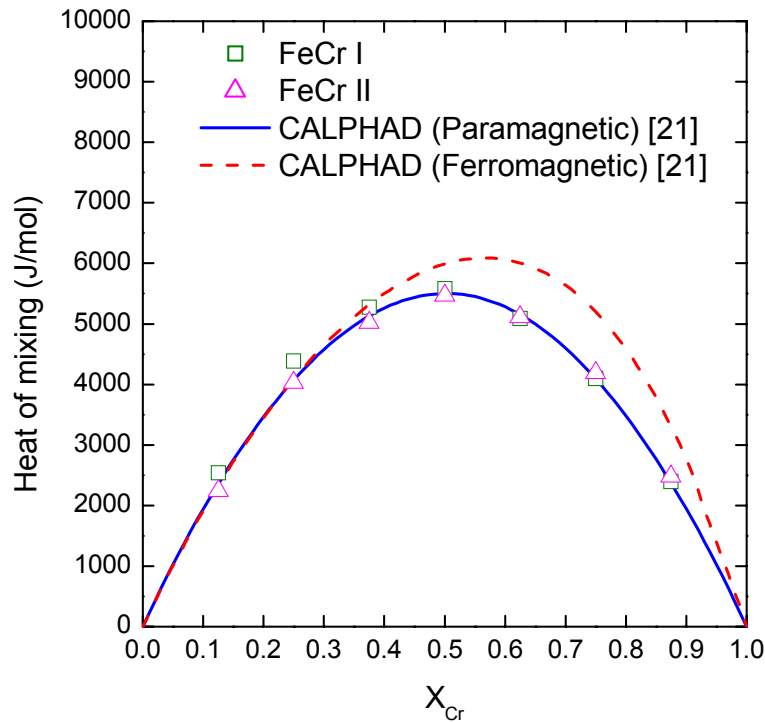


Fig. 2. Calculated heat of mixing in Fe-Cr bcc alloys by the present Fe-Cr potentials in comparison with the CALPHAD calculations.

measured changes in isochronal annealing recovery [34]. Thus, it was decided to fit another Fe-Cr potential, which provided a positive Cr – SIA binding energy, by fitting α and β simultaneously. This potential was named FeCr II. FeCr II does predict positive binding energies for the mixed dumbbells, as shown in Table 2, in addition to also providing good agreement with the enthalpy of mixing and the lattice constants, as shown in Figs. 2 and 3.

In order to validate these two different Fe-Cr potentials, a simple ab-initio calculation was performed using the SeqQuest code [27], which is based on the linear combination of atomic orbitals (LCAO) formulation. A substitutional Cr atom was placed in the bcc Fe matrix consisting of 54 atoms. Although a Cr atom should be slightly oversized compared to Fe, the first nearest neighbor Fe atoms constrict toward the Cr atom by 0.1% in the SeqQuest code. This is in better agreement with the prediction of FeCr II as shown in Table 3 and seems to be closely associated with the stable mixed dumbbells in Fe-Cr alloys predicted by the ab-initio calculation [26]. However, it is not well understood why the mixed dumbbells are energetically stable since Cr is slightly oversized, as well as elastically stiffer than Fe [17]. Possibly, this results from a strong electronic interaction between Fe and Cr atoms in a Fe-rich region, which may also be influenced by magnetic spin effects.

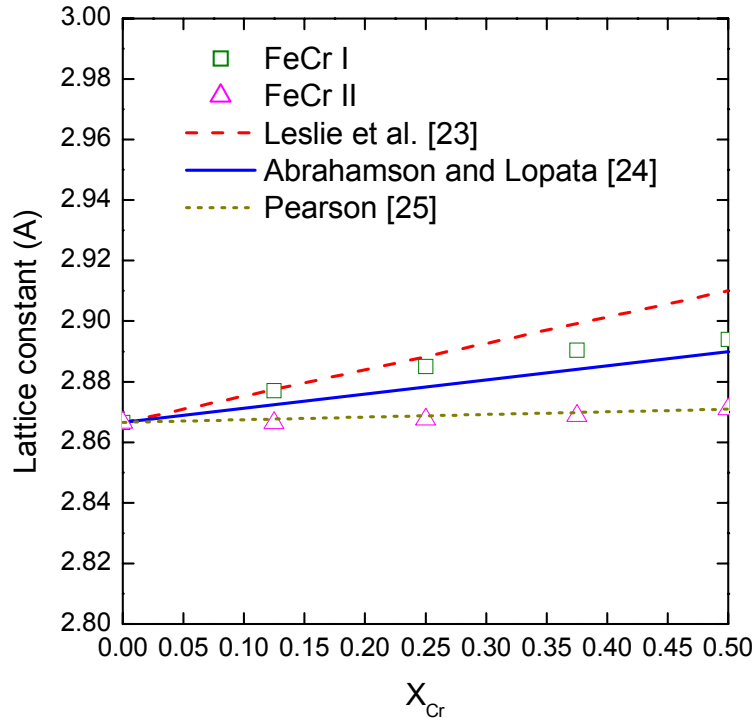


Fig. 3. Calculated lattice constants in Fe-Cr bcc alloys by the present Fe-Cr potentials in comparison with the experimental data.

Table 2. Calculated binding energies of Cr-vacancy, Cr-Cr and Cr-dumbbells in bcc Fe relative to well-separated Cr/vacancy (eV)

	F-S FeCr I	F-S FeCr II	EAM Wallenius [6]	Ab-initio Domain [11]
Cr-V 1NN	0.0386	-0.0016	-	-
Cr-V 2NN	-0.0369	-0.0130	-	-
Cr-Cr 1NN	0.0695	0.0285	-	-
Cr-Cr 2NN	0.0004	0.0289	-	-
$\langle 110 \rangle I_{FeCr}$	-0.4037	0.1015	0.27	0
$\langle 111 \rangle I_{FeCr}$	-0.2540	0.1950	-	0.3
$\langle 110 \rangle I_{FeFe-Cr}$ (parallel)	-0.1634	0.0625	-	-
$\langle 110 \rangle I_{FeFe-Cr}$ (perpendicular)	0.0165	-0.0072	-	-

Table 3. Change in first nearest neighbor distance around a substitutional Cr atom in bcc Fe

	Change (%)
FeCr I	+0.532
FeCr II	-0.316
Ab-initio (SeqQuest)	-0.292

The developed Fe-Cr potentials were implemented in the MDCASK code [28]. The MD simulations were performed using a constant pressure periodic boundary condition based on the Parrinello-Rahman method [29]. The computational cell consisted of 60x60x60 bcc unit cells (432,000 atoms). The cell was thermally equilibrated at 673 K for 30 ps prior to the cascades. The cascades were initiated by giving a primary knock-on atom (PKA) a kinetic energy E_p ranging from 1 to 20 keV along $\langle 135 \rangle$ directions, consistent with the approach of other researchers [1,2], in pure Fe and Fe-10%Cr alloys with both FeCr I and FeCr II. The MD simulations continued for 40 ps after cascade introduction without temperature rescaling. In order to obtain defect production statistics, 5–10 MD simulations were performed at each kinetic energy, while changing the specific PKA directions. The Wigner-Seitz cell method was adopted to analyze the number and distribution of produced defects. Second nearest neighbor (NN) criterion for vacancies and third NN criterion for self-interstitial atoms (SIAs) were used for the definition of clusters.

Results

Figure 4 plots the variation in the average number of Frenkel pairs with time for pure Fe and Fe-10%Cr (FeCr I and FeCr II) for the 20 keV cascades. Very similar behavior is shown for pure Fe and Fe-10%Cr (FeCr I and FeCr II). As seen by other research groups [1,2,4–6], the number of Frenkel pairs increases rapidly until reaching a peak around 0.5 ps after initiating the PKA, during the so-called collision stage. The number of Frenkel pairs at the peak varies between 800 and 900. Following the peak, the number of Frenkel pairs quickly decreases due to the recombination of SIAs and vacancies and then about 5 ps after the cascade start, begins to decrease more slowly.

The average number of Frenkel pairs surviving 40 ps after initiating the cascade is plotted in Fig. 5 as a function of PKA energy, E_p . A similar tendency with the power law for pure Fe proposed by Bacon et al. [30] is observed, though with a smaller prefactor of 3.5 vs. 5.7 and a slightly increased power law exponent of 0.82 vs. 0.78. The defect production efficiency is presented in Fig. 6 by dividing the number of surviving Frenkel pairs into the number of displacements predicted by the Norgett-Robinson-Torrens (NRT) model [31], $0.8E_p/2E_d$. The recommended value of the average threshold displacement energy, E_d , of 40 eV was used for bcc Fe [2]. In agreement with other work [1,2,4,5], the efficiency decreases slowly as E_p increases and remains almost constant from 10 to 20 keV. The asymptotic value is about 0.22, which is slightly lower than the previous works for pure Fe [2] and Fe-10%Cr [5]. These results indicate that Cr atoms in Fe do not have a significant effect on the number of primary irradiation defects forming during cascades.

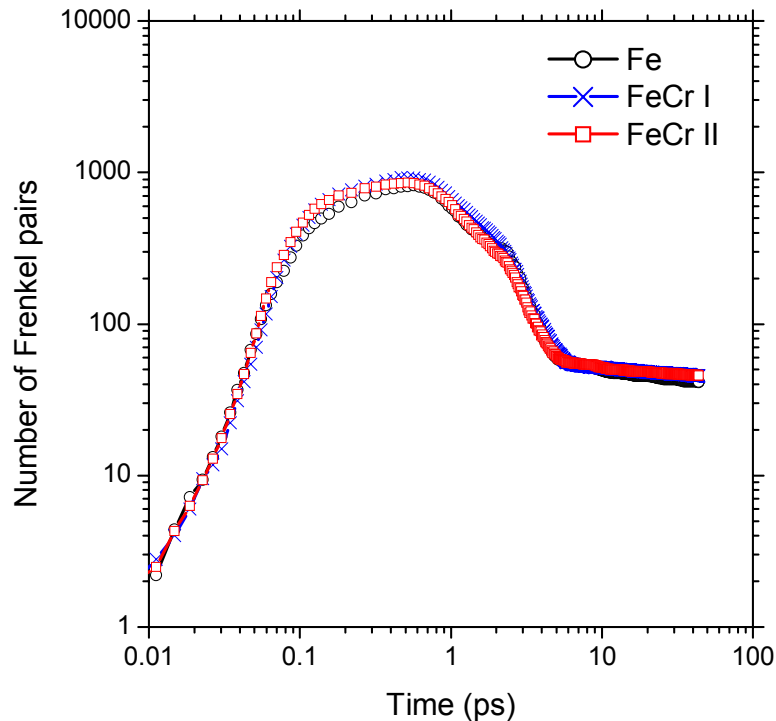


Fig. 4. Number of Frenkel pairs versus time at 20 keV cascades.

Figure 7 shows the typical defect distribution for pure Fe and Fe-10%Cr at 40 ps after initiating the 20 keV cascades. Notably, no significant difference in the defect distribution between pure Fe and Fe-10%Cr is found. While most vacancies are single vacancies, many of the SIAs form clusters containing more than 2 SIAs. Very large clusters containing more than 10 SIAs are often found in all cases. The results from the FeCr I and FeCr II potentials exhibit an opposite feature with respect to the binding (local chemistry) around the defects. As shown in Fig. 8, many Fe-Cr mixed dumbbells (crowdions) and even Cr-Cr dumbbells are produced using the FeCr II potential, whereas mixed dumbbells (crowdions) are not stable in FeCr I and most of the SIA dumbbells involve only Fe atoms. This result is expected from the negative and positive binding energies of the Fe-Cr mixed dumbbell in FeCr I and FeCr II, respectively, as previously shown in Table 2. The fraction of mixed dumbbells observed with the FeCr II potential is larger than that expected of a Fe-10%Cr alloy, assuming that Cr atoms are randomly distributed and there is no interaction between dumbbells and Cr atoms, which would be 0.2 and again, is indicative of the strong binding energy between Cr atoms and SIA from this potential. For the case of larger SIA clusters, Cr atoms are often found associated with the clusters, independent of the choice of interatomic potentials.

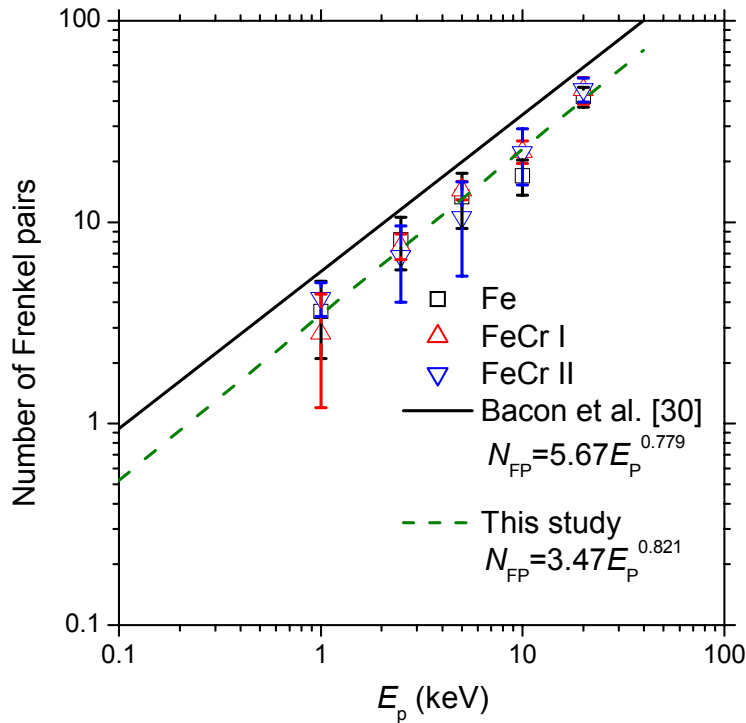


Fig. 5. Number of Frenkel pairs versus E_p .

The results of vacancy and SIA cluster size analysis at 20 keV are summarized in Fig. 9. Consistent with previous work on pure Fe [4], most vacancy clusters consist of 2 and 3 vacancies. In Fe-10%Cr, the number of di-vacancy clusters appears slightly larger than in pure Fe. But, it is not clear at this time whether this is a statistically significant result. For SIA clusters, various cluster sizes are observed, though largest population consists of di-SIA clusters. Figure 10 shows the fractions of vacancies and SIAs in clusters as a function of E_p . The data for vacancy clustering has a large amount of scatter, with cluster fractions varying between 5 and 25%, as Becquart et al. [4] found in their Fe-Cu cascade simulations. The fraction of SIAs in clusters rapidly increases with increasing E_p at the low energy cascades and then exhibits a saturation tendency of about 65% from 5 keV. This tendency is in agreement with pure Fe cascade simulations by Stoller et al. [2] using the original F-S Fe potential. However, the fraction of SIAs in clusters is slightly larger compared to Fe-Cr cascades simulations of Malerba et al. [5]. On the whole, Cr atoms in Fe are unlikely to have a large effect on the clustering tendency of either vacancies or SIA during cascade timescales on the order of tens of picoseconds.

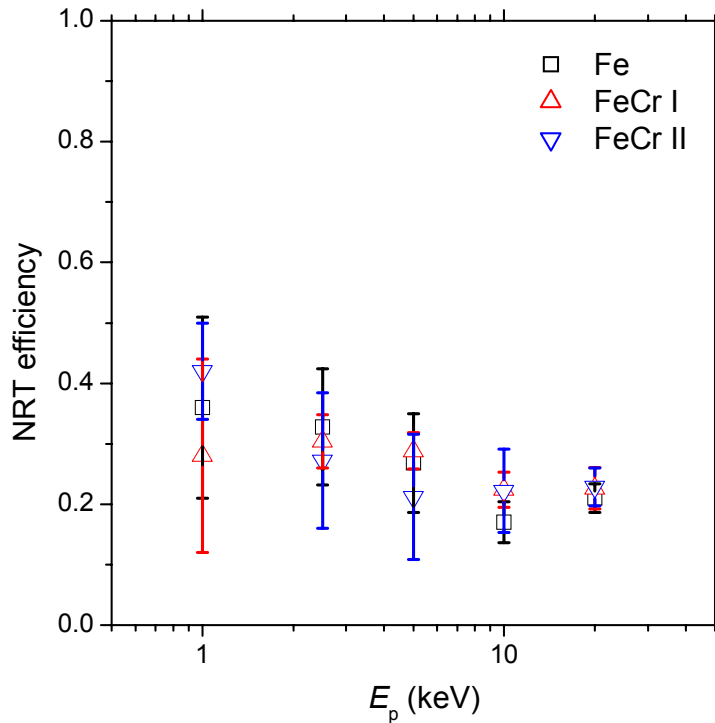
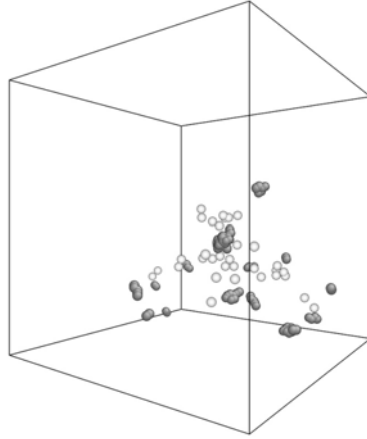


Fig. 6. Defect production efficiency versus E_p .

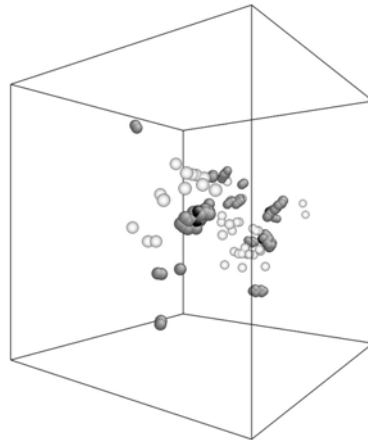
Discussion

In this study, it is found that Cr atoms in Fe do not have a significant effect on the number of defects produced nor on the formation of clusters during cascades, consistent with other cascade simulations of Fe alloys [5,6]. However, the long-time defect formation and the subsequent microstructural evolution during the annealing stages of cascade aging are more likely to be influenced by the presence of Cr atoms, since Cr atoms can have a more significant impact on defect mobility, particularly for single SIAs and SIA clusters. According to recent MD simulations in Fe-Cr [9] and Fe-Cu [32] alloys, the diffusivity of SIAs are influenced by the presence of solute atoms, especially at low temperatures. In addition, there are experimental observations of a small positive binding energy between Cr and self-interstitial atoms in Fe-Cr alloys, including the possible formation of Fe-Cr mixed dumbbells [34] and that Cr atoms retard the one-dimensional motion of interstitial loops in Fe [33]. It is thought that the binding between SIAs and Cr atoms is the main factor controlling the SIA diffusivity. The two interatomic Fe-Cr potentials proposed in this study show opposite binding interactions for Fe-Cr mixed dumbbells. At present it is quite difficult to decide which potential is more accurate, although the recent ab-initio calculations and the experimental work of Maury support FeCr II. Sufficient experimental investigations of the stability of mixed dumbbells, along with models to compare these results to previous experimental studies of isochronal annealing recovery [34,35], are required to further validate these potentials.

Fe



FeCr I



FeCr II

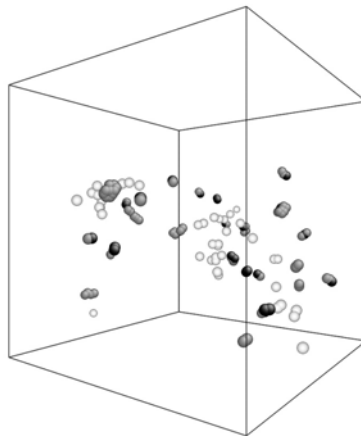


Fig. 7. Typical defect distributions at 40 ps after 20 keV cascades. The empty, gray and black circles represent vacancies, Fe SIAs and Cr SIAs, respectively.

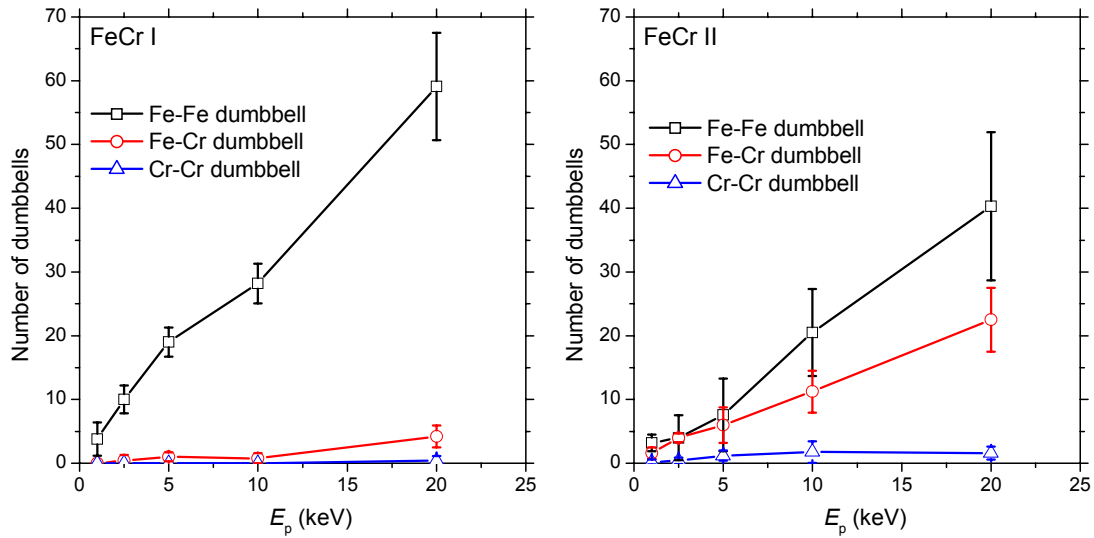


Fig. 8. Number of Fe-Fe, Fe-Cr and Cr-Cr dumbbells in Fe-10%Cr alloys after 20 keV cascades.

Conclusions

MD simulations of displacement cascades with kinetic energy up to 20 keV have been performed in Fe and Fe-10%Cr with potentials based on the Finnis-Sinclair formalism. Two different cross potentials for Fe-Cr, FeCr I and FeCr II are fit to the experimental information available in Fe-Cr alloys, including the heat of mixing and lattice constants. These two potentials exhibit very different behavior for the Cr-SIA interaction; the FeCr I potential predicts unstable Fe-Cr mixed dumbbells while FeCr II predicts stable mixed dumbbells. The potentials used in this study show good agreement, but with slightly lower NRT efficiency than compared to previous works for Fe and Fe-Cr alloys. It is found that Cr atoms do not greatly influence the defect population during the collisional stage of cascades independent of which Fe-Cr potential is selected. However, with FeCr II, many mixed dumbbells are produced after the collisional stage of cascades, well beyond the concentration of Cr. Interesting, the fraction of mixed dumbbells is lower than the results of Malerba et al. [5], possibly due to the lower binding energy derived from the potentials in this work. On the whole, Cr atoms in Fe do not have a significant effect on the production nor distribution of vacancy and SIA clusters right after the collisional cascade stage, independent of the chosen Fe-Cr potential. However, it is expected that the presence of Cr atoms will influence the mobility of SIAs and subsequently damage accumulation and microstructural evolution.

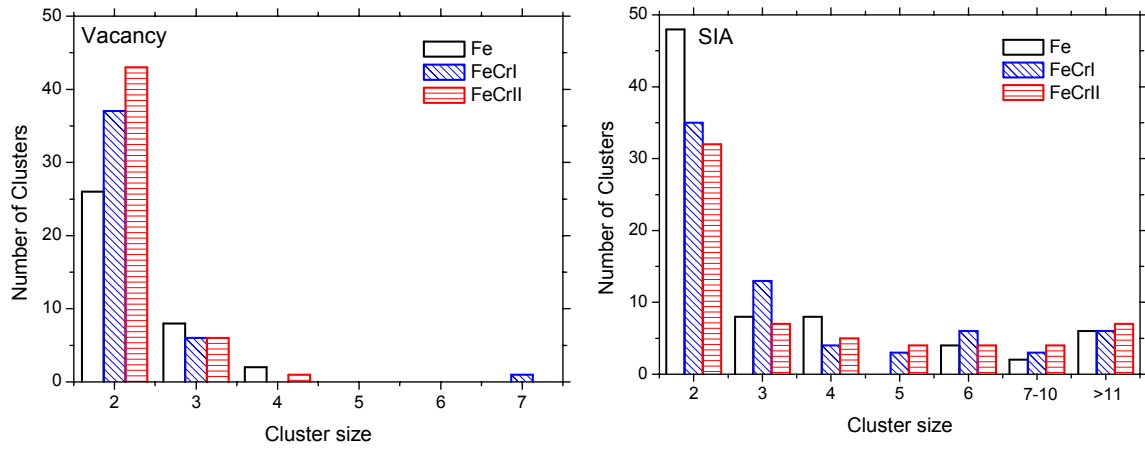


Fig. 9. Size distributions of vacancy and SIA clusters after 20 keV cascades.

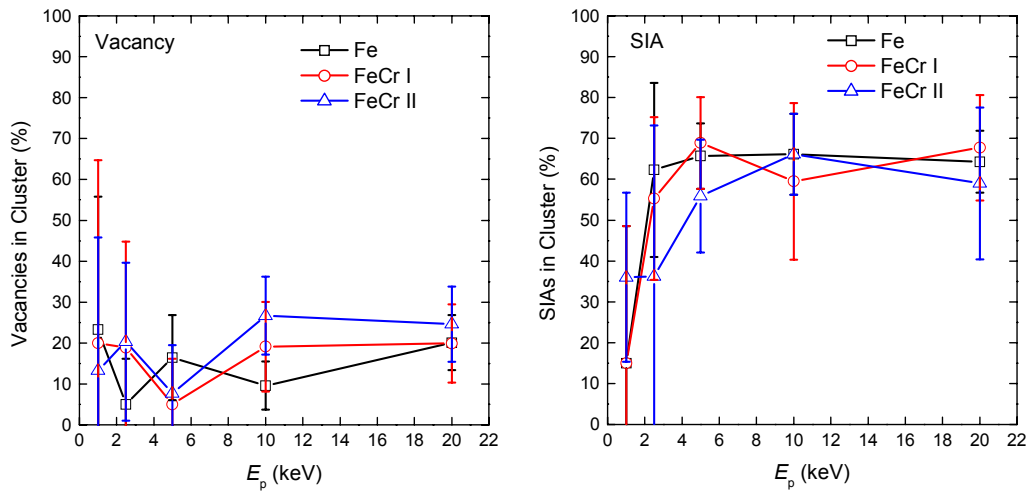


Fig. 10. Fraction of vacancies and SIAs in clusters versus E_p .

Acknowledgements

This work has been supported by the Office of Fusion Energy Sciences, US Department of Energy, under Grant DE-FG02-04ER54750.

References

- [1] A. F. Calder and D. J. Bacon, J. Nucl. Mater. 207 (1993) 25.
- [2] R. E. Stoller, G. R. Odette, and B. D. Wirth, J. Nucl. Mater. 251 (1997) 49.

- [3] N. Soneda and T. Diaz de la Rubia, *Philos. Mag.* A 78 (1998) 995.
- [4] C. S. Becquart, C. Domain, A. Legis, and J. C. Van Duysen, *J. Nucl. Mater.* 280 (2000) 73.
- [5] L. Malerba, D. Terentyev, P. Olsson, R. Chakarova, and J. Wallenius, *J. Nucl. Mater.* 329–333 (2004) 1156.
- [6] J. Wallenius, P. Olsson, C. Lagerstedt, N. Sandbers, R. Chakarova, and V. Pontikis, *Phys. Rev. B.* 69 (2004) 094103.
- [7] M. S. Daw and M. I. Baskes, *Phys. Rev. Lett.* 50 (1983) 1285.
- [8] D. Farkas, C. G. Schon, M. S. F. de Lima, and H. Goldstein, *Acta Mater.* 44 (1996) 409.
- [9] D. Terentyev and L. Malerba, *J. Nucl. Mater.* 329–333 (2004) 1161.
- [10] H. Maeta, F. Ono, and T. Kittaka, *J. Phys. Soc. Japan* 53 (1984) 4353.
- [11] C. Domain and C. S. Becquart, *Phys. Rev. B.* 65 (2001) 024103.
- [12] C.-C. Fu, F. Willaime, and P. Ordejón, *Phys. Rev. Lett.* 92 (2004) 175503.
- [13] B. D. Wirth, G. R. Odette, D. Maroudas, and G. E. Lucas, *J. Nucl. Mater.* 244 (1997) 185.
- [14] G. J. Ackland, D. J. Bacon, A. F. Calder, and T. Harry, *Philos. Mag. A* 75 (1997) 713.
- [15] M. I. Mendeleev, S. Han, D. J. Srolovitz, G. J. Ackland, D. Y. Sun, and M. Asta, *Philos. Mag.* 83 (2003) 3977.
- [16] H. J. Wollenberger, In R. W. Cahn and P. Haasen (eds.), *Phys. Metall.*, Third Edition, Elsevier, Amsterdam (1983) 1139–1221.
- [17] M. W. Finnis and J. E. Sinclair, *Philos. Mag. A* 50 (1984) 45.
- [18] J. H. Rose, J. R. Smith, F. Guinea, and J. Ferrante, *Phys. Rev. B* 29 (1984) 2963.
- [19] T. Konishi, K. Ohsawa, H. Abe, and E. Kuramoto, *Comput. Mater. Sci.* 14 (1999) 108.
- [20] G. J. Ackland and V. Vitek, *Phys. Rev. B* 41 (1990) 10324.
- [21] J.-O. Andersson and B. Sundman, *Calphad* 11 (1987) 83.
- [22] W. A. Dench, *Trans. Faraday Soc.* 59 (1963) 1279.
- [23] W. Leslie, R. J. Sober, S. G. Babcock, and S. J. Green, *Trans. Am. Soc. Metall.* 62 (1969) 690.
- [24] E. P. Abrahamson and S. L. Lopata, *Trans. Metall. Soc. AIME* 236 (1966) 76.
- [25] W. B. Pearson, *A Handbook of Lattice Spacings and Structures of Metals and Alloys*, Pergamon Press, New York (1958) 532.
- [26] C. Domain, (private communication).
- [27] <http://www.cs.sandia.gov/~paschul/Quest>.
- [28] T. Diaz de la Rubia and M. W. Guinan, *J. Nucl. Mater.* 174 (1990) 151.
- [29] M. Parrinello and A. Rahman, *Phys. Rev. Lett.* 45 (1980) 1196.
- [30] D. J. Bacon, A. F. Calder, F. Gao, V. G. Kapinos, and S. J. Wooding, *Nucl. Instrum. Methods B* 102 (1995) 37.
- [31] M. J. Norgett, M. T. Robinson, and I. M. Torrens, *Nucl. Eng. Des.* 33 (1975) 50.
- [32] J. Marian, B. D. Wirth, J. M. Perlado, G. R. Odette, and T. Diaz de la Rubia, *Phys. Rev. B* 64 (2001) 094303.
- [33] K. Arakawa, M. Hatanaka, H. Mori, and K. Ono, *J. Nucl. Mater.* 329–333 (2004) 1194–1198.
- [34] F. Maury, P. Lucasson, A. Lucasson, F. Faudot, and J. Bigot, *J. Phys. F: Met. Phys.* 17 (1987) 1143.
- [35] H. Abe and E. Kuramoto, *J. Nucl. Mater.* 271–272 (1999) 209–213.